

# Supporting information

## Synthesis of Anisotropic Concave Gold Nanocuboids with Distinctive Plasmonic Properties

*Youju Huang,<sup>a, §</sup> Lin Wu,<sup>b, §</sup> Xiaodong Chen,<sup>c</sup> Ping Bai,<sup>b,\*</sup> Dong-Hwan Kim<sup>a,\*</sup>*

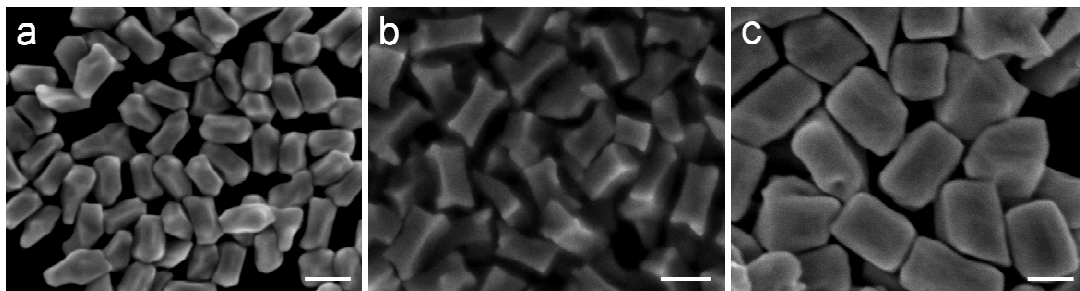
<sup>a</sup> School of Chemical and Biomedical Engineering, and <sup>c</sup> School of Materials Science and Engineering, Nanyang Technological University, 637457, Singapore.

<sup>b</sup> Institute of High Performance Computing, 1 Fusionpolis Way, Singapore 138132

<sup>§</sup>These authors contributed equally to this work.

---

\*Corresponding author: e-mail: [dhkim@ntu.edu.sg](mailto:dhkim@ntu.edu.sg); [baiping@ihpc.a-star.edu.sg](mailto:baiping@ihpc.a-star.edu.sg).



**S-Figure 1.** Representative SEM images of synthesized AuNPs (a), (b) and (c) at the AuNR seed concentrations of  $2\times C_0$ ,  $0.5\times C_0$  and  $0.2\times C_0$  respectively. The scale bars in a, b and c represent 100 nm.

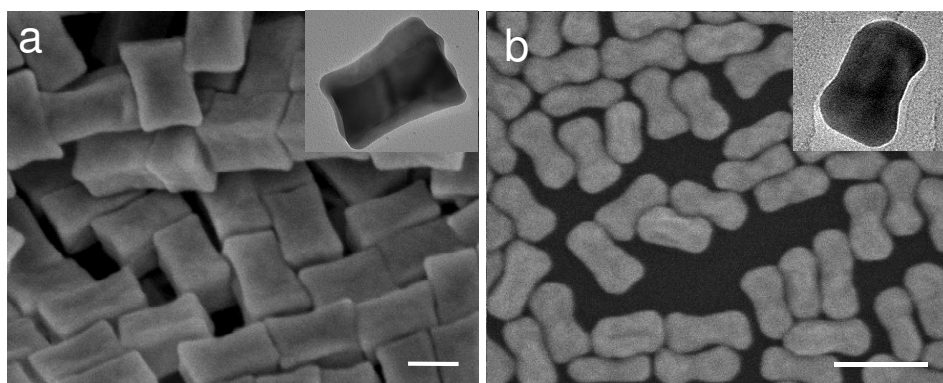
### **Difference between the concave Au nanocuboid and dog bone-like AuNP.**

Here we clarify the difference between our concave Au nanocuboid and dog bone-like AuNP reported previously.

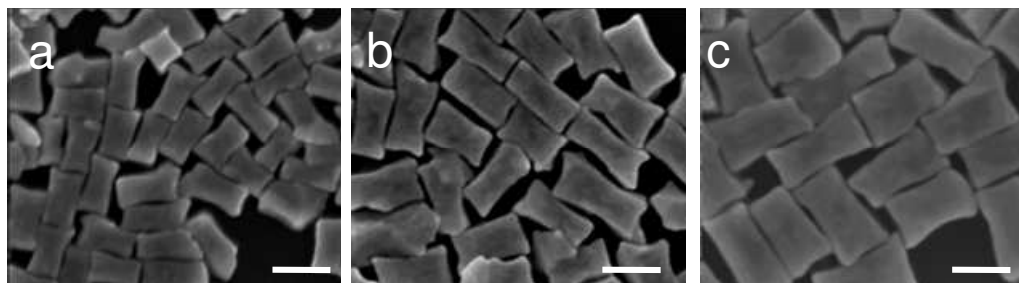
- 1) Shape: Although the concave Au nanocuboid and the dog bone-like AuNP resemble at first glance, the distinctive difference between two AuNPs is the nature of facets. The concave Au nanocuboid possesses concave facets, calculated to be high index facet of [730], whereas the dog bone-like AuNPs<sup>1-3</sup> have low index facets, such as [100] and [110].<sup>4-6</sup> The SEM and TEM image of the concave Au nanocuboid in S-Figure 2a shows sharp edges along the long axis, verified by high thickness contrast between edge and center, while dog bone-like AuNP exhibits no concave facets, indicated by no thickness contrast in TEM image (S-Figure 2b).
- 2) Synthesis method: Besides differences in a number of experimental parameters, the concave Au nanocuboid was synthesized using Au nanorods as a seed, whereas the dog bone-like AuNP was synthesized using small Au nanospheres (about 4 nm).<sup>1-3</sup> Au nanorod seed allows precise kinetic control to achieve site selective overgrowth of metal nanoparticles.<sup>7,8</sup> As a result, we were able to fabricate much bigger nanoparticles (average

length  $\times$  width:  $140 \pm 8 \times 68 \pm 5$  nm) than the dog bone-like AuNP ( $45 \pm 9 \times 22 \pm 6$  nm).

- 3) Optical property: The dog bone-like AuNP shows three absorption peaks measured from an ensemble of particles in solution. Therefore, this data inevitably includes contributions from non-dog bone structures, such as spheres or cubes,<sup>3</sup> the plasmon resonance peaks of which are typically located around 450-600 nm. In the present study, we investigated surface plasmon resonance of a single Au nanoparticle that exhibits three plasmonic peaks. and also theoretically studied the nature of the newly observed third plasmonic resonance by computer simulation.



**S-Figure 2.** SEM images of concave Au nanocuboids (a) and dog bone-like AuNPs (b), insets; TEM images of a single particle in respective SEM images. Scale bars represent 100 nm. dog bone-like AuNPs were synthesized according to the synthesis method described in the literature.<sup>3</sup>

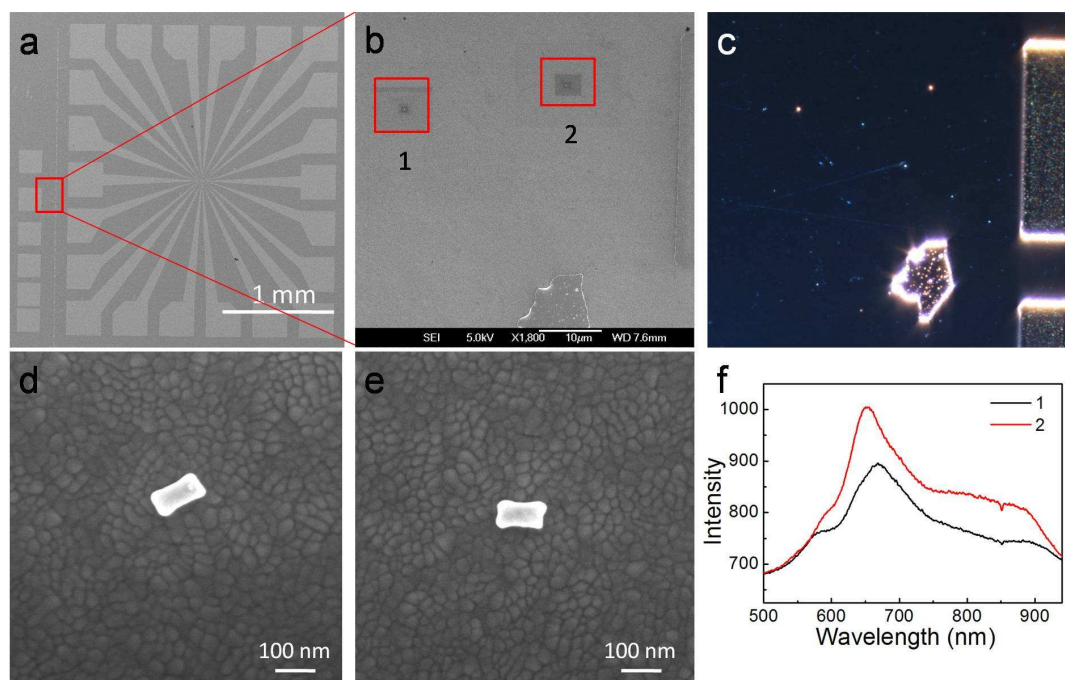


**S-Figure 3.** SEM images of concave Au nanocuboids with different sizes ( $70 \pm 4 \times 40 \pm 2$  (a),  $110 \pm 6 \times 50 \pm 3$  (b) and  $140 \pm 8 \times 68 \pm 5$  (average length  $\times$  width) (c)). Scale bars in represent 100 nm.

### **Pattern matching technique for single particle observation**

Single-nanoparticle set-up has been reported in our previous works.<sup>7,9,10</sup> Briefly, Dark-field imaging and spectroscopy on single nanoparticles were carried out with an Olympus IX71 inverted microscope coupled with a color digital camera (DS-Fi1-U2 with the NIS Element D software) and a line-imaging spectrometer (Acton Research SpectraPro2150i). The system employs an oil (refractive index of 1.516) immersion ultra-dark-field condenser (numerical aperture of 1.2-1.4) and a 100 $\times$  oil immersion Plan-neofluar (Olympus) objective with an adjustable numerical aperture from 0.6 to 1.3. Illumination was provided by an integrated 100 W halogen source.

Based on pattern-matching technique, one-to-one correspondence between SEM and Dark-field images of single nanoparticles were performed. Briefly, gold patterns were printed on a ITO glass (figure S4a). This gold pattern in microns was used as a “land mark” that allows identifying and registering the same nanoparticle between SEM and dark field images. Figure S4d, e and f show their morphology and corresponding LSPR spectra of single gold nanocuboids.



**S-Figure 4.** SEM image of gold pattern on ITO glass; b: enlarged SEM image of a; c: the corresponding optical image of b; d and e: enlarged SEM of gold concave nanocuboids (1 and 2 in b); f: the corresponding localized scattering plasmonic resonance spectra of single gold concave nanocuboids (d and e).

## REFERENCES AND NOTES

- (1) Gou, L.; Murphy, C. J. *Chem. Mater.* **2005**, *17*, 3668.
- (2) Wang, C.; Wang, T.; Ma, Z.; Su, Z. *Nanotechnology* **2005**, *16*, 2555.
- (3) Xu, X.; Cortie, M. B. *Adv. Fuc. Mater.* **2006**, *16*, 2170.
- (4) Wang, Z. L.; Mohamed, M. B.; Link, S.; El-Sayed, M. A. *Surf. Sci.* **1999**, *440*, L809.
- (5) Katz-Boon, H.; Rossouw, C. J.; Weyland, M.; Funston, A. M.; Mulvaney, P.; Etheridge, J. *Nano Lett.* **2011**, *11*, 273.
- (6) Wang, Z. L.; Gao, R. P.; Nikoobakht, B.; El-Sayed, M. A. *J. Phys. Chem. B* **2000**, *104*, 5417.
- (7) Huang, Y.; Kim, D. H. *Nanoscale* **2011**, *3*, 3228.
- (8) Sohn, K.; Kim, F.; Pradel, K. C.; Wu, J.; Peng, Y.; Zhou, F.; Huang, J. *ACS Nano* **2009**, *3*, 2191.
- (9) Guo, L.; Ferhan, A. R.; Chen, H.; Li, C.; Chen, G.; Hong, S.; Kim, D. H. *Small* **2013**, *9*, 234.
- (10) Guo, L.; Ferhan, A. R.; Lee, K.; Kim, D. H. *Anal. Chem.* **2011**, *83*, 2605.